

Supersymmetry and Electroweak Leptonic Observables

Oleg Lebedev¹ and Will Loinaz²

¹Centre for Theoretical Physics, University of Sussex, Brighton BN1 9QJ, UK

²Department of Physics, Amherst College, Amherst MA 01002, USA

Abstract

We study vertex corrections to the leptonic electroweak observables in the general MSSM at $\tan \beta \lesssim 35$. In particular, we address the question of whether supersymmetry can be responsible for the observed 2σ deviation from the Standard Model prediction in the invisible width of the Z . We find that the presence of a light (around 100 GeV) chargino and sleptons hinted by the $g_\mu - 2$ measurements makes the agreement with experiment slightly better and improves the electroweak fit.

1 Introduction

The recent BNL measurements of the muon anomalous magnetic moment have bolstered interest in supersymmetric models [1]. These measurements appear to deviate from Standard Model (SM) predictions by 2.6σ [2]. A conclusive statement can be made only after sufficient statistics have been accumulated and the status of the SM theoretical uncertainties has been determined unambiguously [3]. However, should this deviation persist and its error shrink, new physics would be required to explain it. Among the candidate models for new physics, supersymmetric models seem most promising [2].

In addition to this possible deviation, there are a number of other discrepancies of similar size between the SM predictions and the experimental values of the electroweak observables. In particular, there is a more long-standing A_b “anomaly” [4],[5] which manifests in a 2.7σ deviation of the combined left-right asymmetry in $Z \rightarrow b\bar{b}$ decays measured at LEP and SLD from the SM prediction. It has been argued that such a discrepancy is unlikely to be a result of a statistical deviation (see e.g. the work of Chanowitz in Ref.[4]). The possibility of supersymmetric origin of this “anomaly” will be pursued in a subsequent paper. In addition, there is a 2σ deviation in the invisible width of the Z boson [5], which appears as a deviation of the effective number of neutrinos from three:

$$N_\nu = 2.9835 \pm 0.0083 . \quad (1)$$

Implications of these results for various models of new physics have been considered in Refs.[6]-[9]. In particular, it was found that models with R-parity violating interactions [6], two Higgs doublet models at large $\tan\beta$ [7], models with large extra dimensions [8], and models with an extra gauge $U(1)_{B-3L}$ [9] not only fail to mitigate but in fact exacerbate the problem by generating radiative corrections of the “wrong” sign. This observation has resulted in stringent constraints on such models.

In this study we analyze the effect of R-conserving supersymmetry on electroweak leptonic observables and, in particular, the invisible width of the Z boson. Motivated by the supersymmetric explanation of the BNL $g-2$ “anomaly”, our study is focused on the question whether or not the Z invisible width “anomaly” can be explained with the same mechanism. In our analysis we perform a global fit to all relevant electroweak leptonic observables such as the R-parameters

$$R_l = \frac{\Gamma(Z \rightarrow \text{hadrons})}{\Gamma(Z \rightarrow l^+l^-)} = \frac{N_c \sum(h_{qL}^2 + h_{qR}^2)}{h_{l_L}^2 + h_{l_R}^2},$$

$$R_{\nu/e} = \frac{\Gamma(Z \rightarrow \nu\bar{\nu})}{\Gamma(Z \rightarrow e^+e^-)} = \frac{h_{\nu L}^2}{h_{e_L}^2 + h_{e_R}^2}, \quad (2)$$

the left-right asymmetries

$$A_l = \frac{h_{l_L}^2 - h_{l_R}^2}{h_{l_L}^2 + h_{l_R}^2}, \quad (3)$$

and the forward-backward asymmetries

$$A_{FB}(l) = \frac{3}{4} A_e A_l, \quad (4)$$

where $h_{l_{L,R}}$ are the $Zl_{L,R}l_{L,R}$ couplings and $l = e, \mu, \tau$. The 2σ deviation in $R_{\nu/e}$ is related to the $\sim 2\sigma$ deviation in $\sigma_{\text{had}} = 12\pi\Gamma_e\Gamma_h/m_Z^2\Gamma_Z^2$. We remark that $R_{\nu/e}$ is not measured directly but rather calculated from the Z-line-shape observables. In principle, $R_{\nu/e}$ could be affected by SUSY contributions to $\Gamma(Z \rightarrow \text{hadrons})$; for example, a light bottom squark may improve agreement with experiment [10]. In this work, we concentrate exclusively on the leptonic sector.

We isolate the effect of the vertex corrections which are sensitive to the lepton/chargino-neutralino sector of the MSSM. The oblique corrections are parameterized in our fit but not used to constrain the model due to their significant model-dependence, e.g. they depend sensitively on the Higgs sector, squark masses, etc. In addition, we let $\alpha_s(M_Z)$ float in our fit since its SM value is extracted from R_l . This strategy has been used previously and proven useful in placing generic constraints on complicated models of new physics [6]-[9]. We incorporate the electroweak data reported during summer 2000 conferences in our numerical analysis.

We present general formulae for the vertex corrections in terms of the low-energy quantities such as the chargino masses and mixings, left and right slepton masses, etc. We then impose the condition of the radiative electroweak symmetry breaking and analyze the GUT scale MSSM parameters which improve the electroweak fit. However, we stress

that our conclusions are independent of the assumptions about the high energy structure of the theory and can be formulated purely in terms of the low energy quantities.

An analysis which addresses a somewhat similar question but with an emphasis on the effect of the oblique corrections has recently appeared in Ref.[11]. We also find a partial overlap with earlier work [12].

The paper is organized as follows. In Section 2 we present our SUSY framework. In section 3 we calculate the supersymmetric vertex corrections and study the decoupling behavior of the SUSY contributions. In section 4 we discuss the fit and our numerical results, and in sectio 5 we make concluding remarks. In the Appendix we list our conventions and relevant Passarino-Veltman functions.

2 Supersymmetric Framework

We will study supersymmetric models with the following superpotential

$$W = -\hat{H}_2 \hat{Q}_i Y_u^{ij} \hat{U}_j + \hat{H}_1 \hat{Q}_i Y_d^{ij} \hat{D}_j + \hat{H}_1 \hat{L}_i Y_e^{ij} \hat{E}_j - \mu \hat{H}_1 \hat{H}_2 \quad (5)$$

and the high energy scale soft breaking potential

$$\begin{aligned} V_{SB} = & \left(m_{0\alpha}^L \right)^2 \phi_\alpha^{L\dagger} \phi_\alpha^L + \left(m_{0\alpha}^R \right)^2 \phi_\alpha^{R*} \phi_\alpha^R - (B\mu H_1 H_2 + h.c.) + \left(A_l Y_{ij}^l H_1 \tilde{l}_{Li} \tilde{e}_{Rj}^* \right. \\ & \left. + A_d Y_{ij}^d H_1 \tilde{q}_{Li} \tilde{d}_{Rj}^* - A_u Y_{ij}^u H_2 \tilde{q}_{Li} \tilde{u}_{Rj}^* + h.c. \right) - \frac{1}{2} (M_3 \lambda_3^c \lambda_3^c + M_2 \lambda_2^a \lambda_2^a + M_1 \lambda_1 \lambda_1) , \end{aligned} \quad (6)$$

where $\phi_\alpha^{L(R)}$ denotes all the scalars of the theory which transform under SU(2) as doublets (singlets). We generally allow for nonuniversal gaugino and scalar masses. Note that as a result of the SU(2) symmetry different isospin components of the doublets have the same soft masses at the high energy scale, whereas there is no similar requirement for the singlets. At low energies this degeneracy will be broken by the electroweak effects.

In what follows we use $\tan \beta$, $m_{0\alpha}$, A_α , M_i as input parameters and obtain low energy quantities via the MSSM renormalization group equations (RGE) given in Ref.[13]. We also assume radiative electroweak symmetry breaking, i.e. that the magnitude of the μ parameter is given (at tree level) by

$$|\mu|^2 = \frac{m_{H_1}^2 - m_{H_2}^2 \tan^2 \beta}{\tan^2 \beta - 1} - \frac{1}{2} m_Z^2 . \quad (7)$$

The phase of μ is an input parameter and is RG-invariant.

At low energies the charged gauginos and higgsinos mix, leading to the following mass matrix (we follow the conventions of Ref.[14]; however, we correct their sign error in the superpotential)

$$M_{\chi^+} = \begin{pmatrix} M_2 & \sqrt{2} M_W \sin \beta \\ \sqrt{2} M_W \cos \beta & \mu \end{pmatrix} .$$

This matrix is diagonalized by a biunitary transformation

$$U^* M_{\chi^+} V^{-1} = \text{diag}(m_{\chi_1^+}, m_{\chi_2^+}) , \quad (8)$$

where U and V are unitary matrices. The mass eigenvalues are defined to be non-negative and $m_{\chi_1^+} \geq m_{\chi_2^+}$.

Similarly, for neutralinos we have

$$M_{\chi^0} = \begin{pmatrix} M_1 & 0 & -M_Z \sin \theta_W \cos \beta & M_Z \sin \theta_W \sin \beta \\ 0 & M_2 & M_Z \cos \theta_W \cos \beta & -M_Z \cos \theta_W \sin \beta \\ -M_Z \sin \theta_W \cos \beta & M_Z \cos \theta_W \cos \beta & 0 & -\mu \\ M_Z \sin \theta_W \sin \beta & -M_Z \cos \theta_W \sin \beta & -\mu & 0 \end{pmatrix}.$$

This symmetric matrix is diagonalized by a unitary matrix N ,

$$N^* M_{\chi^0} N^{-1} = \text{diag}(m_{\chi_1^0}, m_{\chi_2^0}, m_{\chi_3^0}, m_{\chi_4^0}), \quad (9)$$

where again the eigenvalues are defined to be non-negative and $m_{\chi_1^0} \geq m_{\chi_2^0} \geq \dots$ The chargino and neutralino spinors can be split into the left and right components in the usual way:

$$\chi_i^+ = \begin{pmatrix} \chi_i^+ \\ \bar{\chi}_i^- \end{pmatrix}, \quad \chi_i^0 = \begin{pmatrix} \chi_i^0 \\ \bar{\chi}_i^0 \end{pmatrix}. \quad (10)$$

Concerning the slepton spectrum, the “left” and “right” charged sleptons also mix at low energies. However, their mixing is proportional to the lepton masses and is negligible unless $\tan \beta$ is very large. Neglecting lepton masses, the low energy mass eigenstates are:

$$\begin{aligned} m_{\tilde{e}_L}^2 &\simeq m_{\tilde{e}}^2 + M_Z^2 \left(-\frac{1}{2} + \sin^2 \theta_W \right) \cos 2\beta, \\ m_{\tilde{e}_R}^2 &\simeq m_{\tilde{e}}^2 - M_Z^2 \sin^2 \theta_W \cos 2\beta, \\ m_{\tilde{\nu}}^2 &\simeq m_{\tilde{e}}^2 + \frac{1}{2} M_Z^2 \cos 2\beta, \end{aligned} \quad (11)$$

where $m_{\tilde{e}}^2$ and $m_{\tilde{\nu}}^2$ are the mass parameters appearing in the low energy analog of Eq.(6).

3 SUSY Vertex Corrections

In this paper we will concentrate on $\tan \beta \lesssim 35$. It is quite difficult to achieve radiative electroweak symmetry breaking for greater $\tan \beta$, so such an assumption can be justified. At $\tan \beta \lesssim 35$ the gauge couplings dominate the lepton Yukawa couplings, so only the gaugino parts of the charginos and neutralinos couple to leptons with an appreciable strength. In addition, one can neglect the left-right slepton mixing in this regime (as will be clear below, each relevant diagram would require two left-right mass insertions, so the effect of this mixing is further suppressed).

We perform our calculations using the two-component spinor technique (see the Appendix for the notation and conventions). The result is expressed as a correction $\delta h_{f_{L,R}}$ to the tree level coupling $h_{f_{L,R}}$ defined by

$$\mathcal{L} = -\frac{g}{\cos \theta_W} Z_\mu \left[h_{f_L} f_L^\dagger \bar{\sigma}^\mu f_L + h_{f_R} f_R^\dagger \sigma^\mu f_R \right], \quad (12)$$

with

$$\begin{aligned} h_{f_L} &= I_3 - Q \sin^2 \theta_W , \\ h_{f_R} &= -Q \sin^2 \theta_W . \end{aligned} \quad (13)$$

Neglecting the lepton Yukawa couplings, we have the following SUSY interactions* [14]

$$\begin{aligned} \mathcal{L}_{\tilde{l}\tilde{\chi}^+} &= -g \left[(U_{11}^* \overline{\chi_1^+} + U_{21}^* \overline{\chi_2^+}) P_L \tilde{\nu}_L + (V_{11}^* \overline{\chi_1^{+c}} + V_{21}^* \overline{\chi_2^{+c}}) P_L e \tilde{\nu}_L^* \right] + h.c. , \\ \mathcal{L}_{\tilde{l}\tilde{\chi}^0} &= -\sqrt{2}g \sum_j \bar{l} P_R \chi_j^0 \tilde{l}_L [I_3 N_{j2} - \tan \theta_W (I_3 - Q) N_{j1}] \\ &\quad + \sqrt{2}g \tan \theta_W \sum_j \bar{l} P_L \chi_j^0 \tilde{l}_R Q N_{j1}^* + h.c. , \\ \mathcal{L}_{Z\chi^+\chi^-} &= \frac{g}{\cos \theta_W} Z_\mu \sum_{ij} \overline{\chi_i^+} \gamma^\mu \left(O_{ij}^{'L} P_L + O_{ij}^{'R} P_R \right) \chi_j^+ , \\ \mathcal{L}_{Z\chi^0\chi^0} &= \frac{g}{2 \cos \theta_W} Z_\mu \sum_{ij} \overline{\chi_i^0} \gamma^\mu \left(O_{ij}^{''L} P_L + O_{ij}^{''R} P_R \right) \chi_j^0 , \\ \mathcal{L}_{Z\bar{l}\bar{l}} &= -\frac{ig}{\cos \theta_W} Z_\mu (I_3 - Q \sin^2 \theta_W) \tilde{l}^* \overset{\leftrightarrow}{\partial}^\mu \tilde{l} . \end{aligned} \quad (14)$$

Here I_3 and Q are the lepton isospin and charge, respectively, and the superscript c stands for a charge conjugated spinor. The vertex structures O_{ij} are given by

$$\begin{aligned} O_{ij}^{'L} &= -V_{i1} V_{j1}^* - \frac{1}{2} V_{i2} V_{j2}^* + \delta_{ij} \sin^2 \theta_W , \\ O_{ij}^{'R} &= -U_{i1}^* U_{j1} - \frac{1}{2} U_{i2}^* U_{j2} + \delta_{ij} \sin^2 \theta_W , \\ O_{ij}^{''L} &= -\frac{1}{2} N_{i3} N_{j3}^* + \frac{1}{2} N_{i4} N_{j4}^* , \\ O_{ij}^{''R} &= -O_{ij}^{''L*} = -O_{ji}^{''L} . \end{aligned} \quad (15)$$

These interactions are to be expressed in terms of the two-component spinors. The implementation is trivial for all interactions except for $\mathcal{L}_{\tilde{l}\tilde{\chi}^+}$, which becomes

$$\mathcal{L}_{\tilde{l}\tilde{\chi}^+} = -g \left[\nu_L^\dagger \left(U_{11} \chi_{1R}^+ + U_{21} \chi_{2R}^+ \right) \tilde{e}_L + e_L^\dagger i\sigma_2 \left(V_{11} (\chi_{1L}^+)^* + V_{21} (\chi_{2L}^+)^* \right) \tilde{\nu}_L \right] + h.c. \quad (16)$$

We remark that χ^+ denotes a Dirac spinor with a positive charge (not to be confused with a hermitian conjugated spinor).

The Z- χ^0 - χ^0 coupling can be simplified by taking advantage of the Majorana nature of the neutralino. For Majorana spinors ψ_1 and ψ_2 we have

$$\overline{\psi_1} \gamma_\mu P_L \psi_2 = -\overline{\psi_2} \gamma_\mu P_R \psi_1 . \quad (17)$$

This corrects an error in Ref.[14] in the expression for the neutralino coupling to right-handed leptons (C77), i.e. N_{j2}^ should be N_{j1}^* .

Using this identity as well as $O_{ij}^{\prime R} = -O_{ji}^{\prime L}$, we obtain

$$\begin{aligned}\mathcal{L}_{Z\chi^0\chi^0} &= \frac{g}{\cos\theta_W} Z_\mu \sum_{ij} \bar{\chi}_{iR}^0 \sigma^\mu O_{ij}^{\prime R} \chi_{jR}^0 \\ &= \frac{g}{\cos\theta_W} Z_\mu \sum_{ij} \bar{\chi}_{iL}^0 \bar{\sigma}^\mu O_{ij}^{\prime L} \chi_{jL}^0.\end{aligned}\quad (18)$$

3.1 Chargino Contributions

In this subsection we list expressions for Feynman diagrams containing charginos in the loop. Since the higgsino coupling to leptons can be neglected at $\tan\beta \lesssim 35$, the charginos induce corrections to the left-handed couplings only. Below we present our results in terms of the corrections to the tree level Z - f_L - f_L couplings h_{f_L} .

$$\begin{aligned}\delta h'_{e_L} : \\ (1a) : & g^2 \sum_{ij} O_{ij}^{\prime L} V_{i1}^* V_{j1} \left[(2-d) \hat{C}_{24} + M_Z^2 \hat{C}_{23} \right] (M_Z^2; m_{\tilde{\nu}}, m_{\chi_i^+}, m_{\chi_j^+}) , \\ (1b) : & g^2 \sum_{ij} O_{ij}^{\prime R} V_{i1}^* V_{j1} m_{\chi_i^+} m_{\chi_j^+} \hat{C}_0 (M_Z^2; m_{\tilde{\nu}}, m_{\chi_i^+}, m_{\chi_j^+}) , \\ (1c) : & -g^2 \sum_k |V_{k1}|^2 \hat{C}_{24} (M_Z^2; m_{\chi_k^+}, m_{\tilde{\nu}}, m_{\tilde{\nu}}) , \\ (1d) : & -g^2 \left(-\frac{1}{2} + \sin^2\theta_W \right) \sum_k |V_{k1}|^2 B_1(0; m_{\chi_k^+}, m_{\tilde{\nu}}) .\end{aligned}\quad (19)$$

Definitions of the B and \hat{C} functions can be found in Appendix B. We note that in addition to Fig. 1d there is another wave function renormalization diagram with the loop on the outgoing electron leg. The corresponding correction is the same as for the diagram in Fig. 1d, so we do not list it separately. The contribution of the wave function renormalization diagrams to the total correction comes with a factor of 1/2, so in effect the total correction is simply given by a sum of individual contributions in Eq.(19). The analogous contribution to the (left-handed) neutrino final state is

$$\begin{aligned}\delta h'_{\nu} : \\ (2a) : & -g^2 \sum_{ij} O_{ij}^{\prime R} U_{j1}^* U_{i1} \left[(2-d) \hat{C}_{24} + M_Z^2 \hat{C}_{23} \right] (M_Z^2; m_{\tilde{e}_L}, m_{\chi_j^+}, m_{\chi_i^+}) , \\ (2b) : & -g^2 \sum_{ij} O_{ij}^{\prime L} U_{j1}^* U_{i1} m_{\chi_i^+} m_{\chi_j^+} \hat{C}_0 (M_Z^2; m_{\tilde{e}_L}, m_{\chi_j^+}, m_{\chi_i^+}) , \\ (2c) : & -g^2 (-1 + 2 \sin^2\theta_W) \sum_k |U_{k1}|^2 \hat{C}_{24} (M_Z^2; m_{\chi_k^+}, m_{\tilde{e}_L}, m_{\tilde{e}_L}) , \\ (2d) : & -\frac{1}{2} g^2 \sum_k |U_{k1}|^2 B_1(0; m_{\chi_k^+}, m_{\tilde{e}_L}) .\end{aligned}\quad (20)$$

The resulting total corrections are

$$\delta h'_{e_L} = g^2 \left[\sum_{ij} O_{ij}^{\prime L} V_{i1}^* V_{j1} \left[(2-d) \hat{C}_{24} + M_Z^2 \hat{C}_{23} \right] (M_Z^2; m_{\tilde{\nu}}, m_{\chi_i^+}, m_{\chi_j^+}) \right.$$

$$\begin{aligned}
& + \sum_{ij} O'{}^R_{ij} V_{i1}^* V_{j1} m_{\chi_i^+} m_{\chi_j^+} \hat{C}_0(M_Z^2; m_{\tilde{\nu}}, m_{\chi_i^+}, m_{\chi_j^+}) \\
& - \sum_k |V_{k1}|^2 \hat{C}_{24}(M_Z^2; m_{\chi_k^+}, m_{\tilde{\nu}}, m_{\tilde{\nu}}) \\
& - \left(-\frac{1}{2} + \sin^2 \theta_W \right) \sum_k |V_{k1}|^2 B_1(0; m_{\chi_k^+}, m_{\tilde{\nu}}) \Big] , \tag{21}
\end{aligned}$$

$$\begin{aligned}
\delta h'_\nu &= -g^2 \left[\sum_{ij} O'{}^R_{ij} U_{j1}^* U_{i1} \left[(2-d) \hat{C}_{24} + M_Z^2 \hat{C}_{23} \right] (M_Z^2; m_{\tilde{e}_L}, m_{\chi_j^+}, m_{\chi_i^+}) \right. \\
& + \sum_{ij} O'{}^L_{ij} U_{j1}^* U_{i1} m_{\chi_i^+} m_{\chi_j^+} \hat{C}_0(M_Z^2; m_{\tilde{e}_L}, m_{\chi_j^+}, m_{\chi_i^+}) \\
& + (-1 + 2 \sin^2 \theta_W) \sum_k |U_{k1}|^2 \hat{C}_{24}(M_Z^2; m_{\chi_k^+}, m_{\tilde{e}_L}, m_{\tilde{e}_L}) \\
& \left. + \frac{1}{2} \sum_k |U_{k1}|^2 B_1(0; m_{\chi_k^+}, m_{\tilde{e}_L}) \right] . \tag{22}
\end{aligned}$$

These corrections are finite as they should be. This can be seen from the relations

$$\begin{aligned}
\sum_{ij} O'{}^L_{ij} V_{i1}^* V_{j1} &= \sum_{ij} O'{}^R_{ij} U_{j1}^* U_{i1} = -1 + \sin^2 \theta_W , \\
\sum_i V_{i1}^* V_{ik} &= \sum_i U_{i1}^* U_{ik} = \delta_{1k}
\end{aligned} \tag{23}$$

and the fact $\text{div}(\hat{C}_{24}) = -1/2 \text{ div}(B_1)$ while \hat{C}_0 and \hat{C}_{23} are finite.

3.2 Neutralino Contributions

Because of their bino component, neutralinos induce corrections to both the left and right couplings of the leptons. Starting with the correction to the right-handed charged lepton coupling, we have

$$\begin{aligned}
& \delta h''_{e_R} : \\
(3a) &: -2g^2 \tan^2 \theta_W \sum_{ij} O''{}^L_{ij} N_{i1}^* N_{j1} \left[(2-d) \hat{C}_{24} + M_Z^2 \hat{C}_{23} \right] (M_Z^2; m_{\tilde{e}_R}, m_{\chi_j^0}, m_{\chi_i^0}) , \\
(3b) &: 2g^2 \tan^2 \theta_W \sum_{ij} O''{}^L_{ij} N_{j1}^* N_{i1} m_{\chi_i^0} m_{\chi_j^0} \hat{C}_0(M_Z^2; m_{\tilde{e}_R}, m_{\chi_i^0}, m_{\chi_j^0}) , \\
(3c) &: -4g^2 \tan^2 \theta_W \sin^2 \theta_W \sum_k |N_{k1}|^2 \hat{C}_{24}(M_Z^2; m_{\chi_k^0}, m_{\tilde{e}_R}, m_{\tilde{e}_R}) , \\
(3d) &: -2g^2 \tan^2 \theta_W \sin^2 \theta_W \sum_k |N_{k1}|^2 B_1(0; m_{\chi_k^0}, m_{\tilde{e}_R}) . \tag{24}
\end{aligned}$$

The corrections to the left-handed charged lepton coupling are given by

$$\begin{aligned}
& \delta h''_{e_L} : \\
(4a) &: -\frac{g^2}{2} \sum_{ij} O''{}^R_{ij} (N_{j2}^* + \tan \theta_W N_{j1}^*)(N_{i2} + \tan \theta_W N_{i1})
\end{aligned}$$

$$\begin{aligned}
& \times \left[(2-d)\hat{C}_{24} + M_Z^2 \hat{C}_{23} \right] (M_Z^2; m_{\tilde{e}_L}, m_{\chi_i^0}, m_{\chi_j^0}) , \\
(4b) : & \frac{g^2}{2} \sum_{ij} O_{ij}^{\prime\prime R} (N_{i2}^* + \tan \theta_W N_{i1}^*) (N_{j2} + \tan \theta_W N_{j1}) \\
& \times m_{\chi_i^0} m_{\chi_j^0} \hat{C}_0 (M_Z^2; m_{\tilde{e}_L}, m_{\chi_i^0}, m_{\chi_j^0}) , \\
(4c) : & -g^2 \left(-\frac{1}{2} + \sin^2 \theta_W \right) \sum_k |N_{k2} + \tan \theta_W N_{k1}|^2 \hat{C}_{24} (M_Z^2; m_{\chi_k^0}, m_{\tilde{e}_L}, m_{\tilde{e}_L}) , \\
(4d) : & -\frac{g^2}{2} \left(-\frac{1}{2} + \sin^2 \theta_W \right) \sum_k |N_{k2} + \tan \theta_W N_{k1}|^2 B_1 (0; m_{\chi_k^0}, m_{\tilde{e}_L}) . \quad (25)
\end{aligned}$$

Finally, the neutrino coupling corrections are

$$\begin{aligned}
& \delta h_\nu'': \\
(5a) : & -\frac{g^2}{2} \sum_{ij} O_{ij}^{\prime\prime R} (N_{j2}^* - \tan \theta_W N_{j1}^*) (N_{i2} - \tan \theta_W N_{i1}) \\
& \times \left[(2-d)\hat{C}_{24} + M_Z^2 \hat{C}_{23} \right] (M_Z^2; m_{\tilde{\nu}}, m_{\chi_j^0}, m_{\chi_i^0}) , \\
(5b) : & \frac{g^2}{2} \sum_{ij} O_{ij}^{\prime\prime R} (N_{i2}^* - \tan \theta_W N_{i1}^*) (N_{j2} - \tan \theta_W N_{j1}) \\
& \times m_{\chi_i^0} m_{\chi_j^0} \hat{C}_0 (M_Z^2; m_{\tilde{\nu}}, m_{\chi_i^0}, m_{\chi_j^0}) , \\
(5c) : & -\frac{g^2}{2} \sum_k |N_{k2} - \tan \theta_W N_{k1}|^2 \hat{C}_{24} (M_Z^2; m_{\chi_k^0}, m_{\tilde{\nu}}, m_{\tilde{\nu}}) , \\
(5d) : & -\frac{g^2}{4} \sum_k |N_{k2} - \tan \theta_W N_{k1}|^2 B_1 (0; m_{\chi_k^0}, m_{\tilde{\nu}}) . \quad (26)
\end{aligned}$$

The total corrections are given by

$$\begin{aligned}
\delta h_{e_R}'' & = -2g^2 \tan^2 \theta_W \left[\sum_{ij} O_{ij}^{\prime\prime L} N_{i1}^* N_{j1} \left[(2-d)\hat{C}_{24} + M_Z^2 \hat{C}_{23} \right] (M_Z^2; m_{\tilde{e}_R}, m_{\chi_j^0}, m_{\chi_i^0}) \right. \\
& - \sum_{ij} O_{ij}^{\prime\prime L} N_{j1}^* N_{i1} m_{\chi_i^0} m_{\chi_j^0} \hat{C}_0 (M_Z^2; m_{\tilde{e}_R}, m_{\chi_i^0}, m_{\chi_j^0}) \\
& \left. + \sin^2 \theta_W \sum_k |N_{k1}|^2 \left\{ 2\hat{C}_{24} (M_Z^2; m_{\chi_k^0}, m_{\tilde{e}_R}, m_{\tilde{e}_R}) + B_1 (0; m_{\chi_k^0}, m_{\tilde{e}_R}) \right\} \right] . \quad (27)
\end{aligned}$$

$$\begin{aligned}
\delta h_{e_L}'' & = -\frac{g^2}{2} \left[\sum_{ij} O_{ij}^{\prime\prime R} (N_{j2}^* + \tan \theta_W N_{j1}^*) (N_{i2} + \tan \theta_W N_{i1}) \right. \\
& \times \left[(2-d)\hat{C}_{24} + M_Z^2 \hat{C}_{23} \right] (M_Z^2; m_{\tilde{e}_L}, m_{\chi_j^0}, m_{\chi_i^0}) \\
& - \sum_{ij} O_{ij}^{\prime\prime R} (N_{i2}^* + \tan \theta_W N_{i1}^*) (N_{j2} + \tan \theta_W N_{j1}) \\
& \times m_{\chi_i^0} m_{\chi_j^0} \hat{C}_0 (M_Z^2; m_{\tilde{e}_L}, m_{\chi_i^0}, m_{\chi_j^0}) + \left(-\frac{1}{2} + \sin^2 \theta_W \right) \sum_k |N_{k2} + \tan \theta_W N_{k1}|^2 \\
& \times \left. \left\{ 2\hat{C}_{24} (M_Z^2; m_{\chi_k^0}, m_{\tilde{e}_L}, m_{\tilde{e}_L}) + B_1 (0; m_{\chi_k^0}, m_{\tilde{e}_L}) \right\} \right] . \quad (28)
\end{aligned}$$

$$\begin{aligned}
\delta h''_\nu &= -\frac{g^2}{2} \left[\sum_{ij} O''^R_{ij} (N_{j2}^* - \tan \theta_W N_{j1}^*) (N_{i2} - \tan \theta_W N_{i1}) \right. \\
&\quad \times \left. \left[(2-d) \hat{C}_{24} + M_Z^2 \hat{C}_{23} \right] (M_Z^2; m_{\tilde{\nu}}, m_{\chi_j^0}, m_{\chi_i^0}) \right. \\
&\quad - \sum_{ij} O''^R_{ij} (N_{i2}^* - \tan \theta_W N_{i1}) (N_{j2} - \tan \theta_W N_{j1}) m_{\chi_i^0} m_{\chi_j^0} \hat{C}_0 (M_Z^2; m_{\tilde{\nu}}, m_{\chi_i^0}, m_{\chi_j^0}) \\
&\quad \left. + \frac{1}{2} \sum_k |N_{k2} - \tan \theta_W N_{k1}|^2 \left\{ 2 \hat{C}_{24} (M_Z^2; m_{\chi_k^0}, m_{\tilde{\nu}}, m_{\tilde{\nu}}) + B_1 (0; m_{\chi_k^0}, m_{\tilde{\nu}}) \right\} \right]. \quad (29)
\end{aligned}$$

These expressions are finite due to the relations

$$\begin{aligned}
\sum_{ij} O''^L_{ij} N_{ik}^* N_{jl} &= 0 \quad , \quad (k, l = 1, 2) , \\
\sum_{ij} O''^R_{ij} N_{jk}^* N_{il} &= 0
\end{aligned} \quad (30)$$

and the fact that the combination $2\hat{C}_{24} + B_1$ is finite. Note that the diagrams in Figs. 3a, 4a, 5a are individually finite. The reason is transparent in the weak eigenstates basis: only the higgsinos couple to Z, and we retain only the gaugino coupling to the leptons, so a mass insertion is necessary on each fermion line to complete the diagram.

3.3 Decoupling of Heavy Superpartners

In this subsection we demonstrate explicitly the decoupling of heavy SUSY particles. As the SUSY mass scale increases, the gauginos and higgsinos become approximate mass eigenstates and V, U can be chosen such that

$$\begin{aligned}
V_{ij} &\rightarrow \delta_{ij} + \mathcal{O} \left(\frac{M_Z}{m_{susy}} \right) , \quad U_{ij} \rightarrow \delta_{ij} + \mathcal{O} \left(\frac{M_Z}{m_{susy}} \right) , \\
O'^L_{ij} &\rightarrow \left(-1 + \sin^2 \theta_W \right) \delta_{i1} \delta_{j1} + \left(-\frac{1}{2} + \sin^2 \theta_W \right) \delta_{i2} \delta_{j2} + \mathcal{O} \left(\frac{M_Z}{m_{susy}} \right) , \\
O'^R_{ij} &\rightarrow \left(-1 + \sin^2 \theta_W \right) \delta_{i1} \delta_{j1} + \left(-\frac{1}{2} + \sin^2 \theta_W \right) \delta_{i2} \delta_{j2} + \mathcal{O} \left(\frac{M_Z}{m_{susy}} \right) .
\end{aligned} \quad (31)$$

In the expressions for the vertex structures O'_{ij} , the factors in front of the Kronecker delta symbols represent the gaugino and higgsino couplings to the Z boson. It is clear that O'_{11} corresponds to the gaugino (\tilde{W}^-) Z coupling, while O'_{22} corresponds to that of the higgsino (\tilde{h}^-). Since O'_{ij} is to be contracted with $V_{il}^* V_{j1}$, the higgsino component drops out of all expressions in the decoupling limit, as expected. Denoting by m a heavy scalar mass and by M a heavy fermion mass, we can rewrite $\delta h'_{e_L}$ as

$$\begin{aligned}
\delta h'_{e_L} &= g^2 \sin^2 \theta_W \left\{ \left[(2-d) \hat{C}_{24} + M_Z^2 \hat{C}_{23} \right] (0; m, M, M) + M^2 \hat{C}_0 (0; m, M, M) \right. \\
&\quad \left. - B_1 (0; M, m) \right\} - g^2 \left\{ \left[(2-d) \hat{C}_{24} + M_Z^2 \hat{C}_{23} \right] (0; m, M, M) \right.
\end{aligned}$$

$$\begin{aligned}
& + M^2 \hat{C}_0(0; m, M, M) + \hat{C}_{24}(0; M, m, m) - \frac{1}{2} B_1(0; M, m) \Big\} + \mathcal{O} \left(\frac{M_Z}{m_{susy}} \right) \\
& \longrightarrow 0.
\end{aligned} \tag{32}$$

Each of the expressions in the curly brackets vanishes, see Appendix B. Note that the decoupling is slow – it is only linear in m_{susy} . Similarly, for the neutrino final state we have

$$\begin{aligned}
\delta h'_\nu &= -g^2 \sin^2 \theta_W \Big\{ [(2-d) \hat{C}_{24} + M_Z^2 \hat{C}_{23}] (0; m, M, M) + M^2 \hat{C}_0(0; m, M, M) \\
&+ 2 \hat{C}_{24}(0; M, m, m) \Big\} + g^2 \Big\{ [(2-d) \hat{C}_{24} + M_Z^2 \hat{C}_{23}] (0; m, M, M) \\
&+ M^2 \hat{C}_0(0; m, M, M) + \hat{C}_{24}(0; M, m, m) - \frac{1}{2} B_1(0; M, m) \Big\} + \mathcal{O} \left(\frac{M_Z}{m_{susy}} \right) \\
&\longrightarrow 0.
\end{aligned} \tag{33}$$

Concerning the neutralino contributions, let us first consider $\delta h''_{e_R}$. Since the mixing between the gauginos and higgsinos vanishes in the decoupling limit, we have

$$\begin{aligned}
N_{i1} &\rightarrow \delta_{i1} + \mathcal{O} \left(\frac{M_Z}{m_{susy}} \right) , \\
O''_{ij} &\rightarrow \mathcal{O} \left(\frac{M_Z}{m_{susy}} \right) \quad \text{for } i, j \neq 3, 4 .
\end{aligned} \tag{34}$$

As a result, the combination $O''_{ij} N_{i1}^* N_{j1}$ vanishes in this limit. Therefore

$$\delta h''_{e_R} = -2g^2 \tan^2 \theta_W \sin^2 \theta_W \Big\{ 2 \hat{C}_{24}(0; M, m, m) + B_1(0; M, m) \Big\} + \mathcal{O} \left(\frac{M_Z}{m_{susy}} \right) \rightarrow 0 .$$

Again, the combination in the curly brackets vanishes (see Appendix B). The same arguments are valid for the neutralino corrections to the couplings of the left-handed leptons.

4 Numerical Analysis

To separate out the effect of vertex corrections, we pursue the strategy of Refs.[6]-[9],[15]. That is, we utilize only those observables which can be expressed as ratios of the weak couplings. The effect of oblique corrections [16] then either cancels in the ratios or can be absorbed into effective $\sin^2 \theta_W$. In the fit, we leave $\sin^2 \theta_W$ as a free parameter and parameterize the vertex corrections as δh_ν , δh_{l_L} , and δh_{l_R} . In addition, we retain $\alpha_s(M_Z)$ as a free parameter since its value is determined from R_l . The fit value of $\delta(\sin^2 \theta_W)$ is not used for constraining the model due to its model dependence. Specifically, $\delta(\sin^2 \theta_W)$ depends on the Higgs, squark, etc. masses and thus is not particularly useful in our general analysis.

We impose the following (direct search) constraints on the SUSY spectrum [17]:

$$\begin{aligned}
m_{\tilde{e}} &\geq 99 \text{ GeV} , \\
m_{\tilde{\mu}} &\geq 96 \text{ GeV} , \\
m_{\tilde{\tau}} &\geq 87 \text{ GeV} , \\
m_{\tilde{\nu}} &\geq 43 \text{ GeV} , \\
m_{\chi^0} &\geq 36 \text{ GeV} , \\
m_{\chi^+} &\geq 94 \text{ GeV} .
\end{aligned} \tag{35}$$

We assume that the lepton parameters are generation-independent since lepton-universality breaking corrections are quite constrained (see, for example, the second reference in [6]); in any case this assumption is not important for our analysis.

Numerically $R_{\nu/e}$ is sensitive to the vertex corrections δh_i and much less sensitive to the oblique corrections:

$$\delta R_{\nu/e} = 7.96 \delta h_{\nu} + 8.50 \delta h_{e_L} - 7.33 \delta h_{e_R} + 1.17 \delta s^2 , \tag{36}$$

where $s^2 \equiv \sin^2 \theta_W$. Similarly, for the left-right asymmetries we have

$$\delta A_e = -3.64 \delta h_{e_L} - 4.23 \delta h_{e_R} - 7.87 \delta s^2 . \tag{37}$$

Since the SM prediction for $R_{\nu/e}$ is above the measured value whereas that for the lepton asymmetries is below the measured values, $\delta h_{e_L} < 0$ is favored by both $R_{\nu/e}$ and A_i, A_{FB} . As shown below, δh_{e_L} in the MSSM is typically larger than δh_{ν} and δh_{e_R} . To get a feeling for the value for δh_{e_L} preferred by the fit, set $\delta h_{\nu} = \delta h_{e_R} = 0$ and fit R_i, A_i, A_{FB} with three parameters: δh_{e_L} , $\delta \alpha_s$, and δs^2 . The best-fit values are

$$\begin{aligned}
\delta h_{e_L} &= -0.00165 \pm 0.00096 , \\
\delta \alpha_s &= 0.024 \pm 0.014 , \\
\delta s^2 &= -0.0002 \pm 0.0005 .
\end{aligned} \tag{38}$$

$R_{\nu/e}$ strongly pulls δh_{e_L} to be negative, resulting in a large correction to R_l which is in turn compensated by a large $\delta \alpha_s$. In addition to a genuine shift in α_s , our “effective” $\delta \alpha_s$ parametrizes potential corrections to $\Gamma(Z \rightarrow \text{hadrons})$ from the squark/Higgs sectors. This is, of course, just a “toy” fit. As we will see below, for a viable MSSM model all the shifts are much smaller. Qualitatively, however, the picture remains the same – a negative δh_{e_L} is preferred by the data.

Consider now the lepton vertex corrections in the MSSM. In Figs.6-9 we display the vertex corrections δh_{ν} , δh_{e_L} , and δh_{e_R} as functions of M_2 and $\tan \beta$. Note that δh_{ν} and δh_{e_L} are quite sensitive to M_2 , whereas its effect on δh_{e_R} is negligible as it arises only via the RG running. In most of the parameter space, δh_{e_L} dominates the other corrections; it has the right sign (negative) to mitigate the invisible width “anomaly”, especially for the positive sign of the μ -term (which is also preferred by the $g_{\mu} - 2$ measurement). We find that the regions of the parameter space where SUSY contributions improve the agreement

	$M_2 = 150$	$M_2 = 170$	$M_2 = 190$	$M_2 = 210$
χ^2	11.09	11.30	11.40	11.48
$\delta\alpha_s \times 10^3$	3.9 ± 3.9	3.4 ± 3.9	3.1 ± 3.9	2.8 ± 3.9
$\delta s^2 \times 10^4$	-9.9 ± 2.0	-10.1 ± 2.0	-10.2 ± 2.0	-10.3 ± 2.0

Table 1: The quality of the fit χ^2 as a function of the GUT scale parameter M_2 (GeV). For comparison, the Standard Model gives $\chi^2 = 11.44$ (d.o.f.=12-2). The corresponding fit values of α_s and $\sin^2 \theta_W$ are also displayed. The other GUT scale parameters are $m_{\tilde{l}} = 10$ GeV, $m_{\tilde{e}} = 85$ GeV, $M_1 = 100$ GeV, $M_3 = 150$ GeV, $A = 100$ GeV, $\tan \beta = 5$ and the scalar mass parameter (except for sleptons) is set to 100 GeV.

with the measured values of $g_\mu - 2$ and $R_{\nu/e}$ are generally compatible, see for instance Ref.[18].

In Figs. 10 and 11, we display the corresponding shifts in $R_{\nu/e}$ as functions of M_2 and $\tan \beta$ (keeping $\sin^2 \theta_W$ fixed). Varying M_2 from 135 to 250 GeV corresponds to varying the light chargino mass from 95 to 180 GeV. Fig. 12 shows the dependence of $R_{\nu/e}$ on the GUT left slepton mass parameter $m_{\tilde{l}}$; its range 10-200 GeV translates into the slepton mass $m_{\tilde{e}_L}$ range of 104-225 GeV.

The error bar for $R_{\nu/e}$ is 0.008 (see Table 2), so the supersymmetric contributions can only be responsible for the shift of about 0.2σ . This suppression results partly from the cancellation between the neutrino and left-handed electron contributions. Indeed, if the chargino is a pure gaugino and the sneutrino and left selectron masses are equal, $\delta h_\nu = -\delta h_{e_L}$ in the $M_Z \rightarrow 0$ approximation and the resulting contribution to $R_{\nu/e}$ is very small (Eq.36). Alternately, if the chargino is a pure higgsino, the corresponding couplings are very much suppressed and the resulting $\delta R_{\nu/e}$ is negligible. One thus expects the largest correction when there is a large splitting between the sneutrino and left selectron masses (which is severely bounded by the SU(2) symmetry) and/or when the chargino is a gaugino-higgsino mixture ($M_2/\mu \sim 1$) [†].

The dependence on other input parameters is significantly weaker. An increase in M_3 affects the μ -term via the radiative EW symmetry breaking condition, which in turn results in heavier charginos and neutralinos. The effect of M_1 is not significant due to the subdominant role of the neutralino contributions. For the same reason the dependence on the masses of the right sleptons is weak.

For completeness, below we provide representative low energy parameters for our studies. The GUT scale parameters $m_{\tilde{l}} = 10$ GeV, $m_{\tilde{e}} = 85$ GeV, $m_0 = 100$ GeV, $M_1 = 100$ GeV, $M_2 = 135$ GeV, $M_3 = 200$ GeV, $A = 100$ GeV, $\phi_\mu = 0$, where m_0 is the mass parameter for the scalars other than sleptons, lead to the following low energy spectrum

$$m_{\chi_i^+} \simeq (372, 95) \text{ GeV} , \quad m_{\chi_i^0} \simeq (374, 353, 96, 38) \text{ GeV} , \\ m_{\tilde{\nu}} \simeq 75 \text{ GeV} , \quad m_{\tilde{e}_L} \simeq 104 \text{ GeV} , \quad m_{\tilde{e}_R} \simeq 101 \text{ GeV} ,$$

[†]This was also noted in Ref.[11]

and the following mixing matrices

$$U = \begin{pmatrix} 0.34 & 0.94 \\ 0.94 & -0.34 \end{pmatrix}, \quad V = \begin{pmatrix} 0.19 & 0.98 \\ 0.98 & -0.19 \end{pmatrix},$$

$$N = \begin{pmatrix} 0.11 & -0.26 & -0.67 & 0.69 \\ 0.05i & -0.08i & -0.70i & -0.71i \\ 0.15 & 0.95 & -0.22 & 0.12 \\ -0.98 & 0.11 & -0.15 & 0.06 \end{pmatrix}. \quad (39)$$

We now turn to the discussion of the fit. In Table 1 we present our fit results for different values of M_2 . That is, we fix the lepton vertex corrections using our GUT parameters in the fit and calculate the corresponding χ^2 (d.o.f.= 12-2). The parameters δs^2 and (effective) $\delta\alpha_s$ are left as free fit parameters, which means that the Higgs and the squark sectors “adjust” themselves so as to give the best fit results.

To determine if there is any improvement over the SM, we perform a fit for the SM under the *same circumstances*, i.e. lepton vertex corrections set to zero, δs^2 and $\delta\alpha_s$ free to account for a variation in the Higgs mass and α_s . The Standard Model fit gives

$$\begin{aligned} \chi^2 &= 11.44 \text{ (d.o.f. = 12 - 2)}, \\ \delta\alpha_s &= 0.0020 \pm 0.0039, \\ \delta s^2 &= -0.00103 \pm 0.00020. \end{aligned} \quad (40)$$

If the chargino is light (100 GeV), the MSSM fit gives $\chi^2 = 11.09$. We see that the SUSY vertex corrections indeed improve the fit due to the improvement in $R_{\nu/e}$ and the lepton asymmetries. The quality of the fit quickly approaches that of the SM as the chargino mass increases. We note that the best fit value of δs^2 for both the SM and the MSSM significantly deviates from zero because of the SLD asymmetries, which signifies that the light Higgs is preferred.

5 Conclusions

We have analyzed leptonic electroweak observables in the general MSSM. We find that supersymmetry can mitigate some of the discrepancies between the Standard Model predictions and the observed values. Namely, it produces vertex corrections of the right sign to improve agreement with $R_{\nu/e}$ and the leptonic asymmetries. As a result, the electroweak fit is improved from $\chi^2 = 11.44$ (SM) to $\chi^2 = 11.09$ (MSSM). This required a light (~ 100 GeV) chargino and relatively light (100-250 GeV) sleptons.

Although the improvement from statistical point of view is not very significant, it is quite encouraging since in the same region of the parameter space the $g_\mu - 2$ discrepancy is also mitigated. This is to be contrasted with a number of “new physics” models considered earlier [6]-[9], all of which made the electroweak fit worse. The improvement of the fit requires light superpartners which can be detected in collider experiments in the near future.

Acknowledgements. The authors are indebted to G. Kane and T. Takeuchi for very helpful discussions and suggestions.

A Appendix: Notation and Conventions

We use the following (chiral) representation of the Dirac matrices:

$$\gamma_\mu = \begin{pmatrix} 0 & \sigma_\mu \\ \bar{\sigma}_\mu & 0 \end{pmatrix}, \quad \gamma_5 = i\gamma^0\gamma^1\gamma^2\gamma^3 = \begin{pmatrix} -\mathbf{1} & 0 \\ 0 & \mathbf{1} \end{pmatrix}, \quad (41)$$

where $\sigma^\mu = (1, \vec{\sigma})$ and $\bar{\sigma}^\mu = (1, -\vec{\sigma})$. The left and right components of a Dirac spinor and the corresponding projectors are defined by

$$\psi \equiv \begin{pmatrix} \psi_L \\ \psi_R \end{pmatrix}, \quad P_{L,R} \equiv \frac{1}{2}(1 \mp \gamma_5). \quad (42)$$

The charge conjugated spinor is given by

$$\psi^c = C\bar{\psi}^T, \quad C = -i\gamma^2\gamma^0, \quad \bar{\psi} \equiv \psi^\dagger\gamma^0. \quad (43)$$

In terms of the two-component spinors this corresponds to

$$\psi^c = \begin{pmatrix} -i\sigma^2\psi_R^* \\ i\sigma^2\psi_L^* \end{pmatrix}, \quad \overline{\psi^c} = \left(\psi_L^T(-i\sigma^2), \psi_R^T(i\sigma^2) \right). \quad (44)$$

Free fermions satisfy the following Dirac equation in the two-component notation

$$\begin{aligned} (k \cdot \bar{\sigma}) \psi_L &= m \psi_R, \\ (k \cdot \sigma) \psi_R &= m \psi_L, \end{aligned} \quad (45)$$

The corresponding propagators read

$$\begin{aligned} \langle \psi_L \psi_L^\dagger \rangle &= i \frac{k \cdot \sigma}{k^2 - m^2}, \quad \langle \psi_R \psi_R^\dagger \rangle = i \frac{k \cdot \bar{\sigma}}{k^2 - m^2}, \\ \langle \psi_L \psi_R^\dagger \rangle &= \langle \psi_R \psi_L^\dagger \rangle = i \frac{m}{k^2 - m^2}. \end{aligned} \quad (46)$$

The following identities are useful for calculating Feynman diagrams in terms of the two-component spinors:

$$\begin{aligned} \sigma^2 \sigma_\mu^T \sigma^2 &= \bar{\sigma}_\mu, \quad \sigma^2 \bar{\sigma}_\mu^T \sigma^2 = \sigma_\mu, \\ \bar{\sigma}^\nu \sigma^\mu \bar{\sigma}_\nu &= (2-d) \bar{\sigma}^\mu, \\ (p \cdot \bar{\sigma}) \sigma^\mu (p \cdot \bar{\sigma}) &= -p^2 \bar{\sigma}^\mu. \end{aligned} \quad (47)$$

B Feynman Integrals

Here we make explicit our notation for the scalar and tensor integrals that appear in the calculation. The definitions of the integrals are slightly different from those of Ref. [19]. The hat on the tensor integrals serves as a reminder of these differences.

B.1 Scalar Integrals

We define the functions B_0 and \hat{C}_0 by:

$$\begin{aligned} B_0 [p^2; m_1, m_2] &\equiv i \mu^{4-d} \int \frac{d^d k}{(2\pi)^d} \frac{1}{(k^2 - m_1^2) [(k+p)^2 - m_2^2]}, \\ \hat{C}_0 [p^2, q^2, (p-q)^2; m_1, m_2, m_3] &\equiv i \int \frac{d^4 k}{(2\pi)^4} \frac{1}{(k^2 - m_1^2) [(k+p)^2 - m_2^2] [(k+q)^2 - m_3^2]}. \end{aligned} \quad (48)$$

The general form of B_0 is given by

$$B_0 [p^2; m_1, m_2] = \frac{-1}{(4\pi)^2} \left[\Delta_\epsilon - \frac{m_1^2 \ln(m_1^2/\mu^2) - m_2^2 \ln(m_2^2/\mu^2)}{m_1^2 - m_2^2} + 1 + F(p^2; m_1, m_2) \right],$$

where $\Delta_\epsilon = \frac{2}{4-d} - \gamma_E + \ln 4\pi$, and [20]

$$\begin{aligned} F(p^2; m_1, m_2) &= 1 + \frac{1}{2} \left(\frac{\Sigma}{\Delta} - \Delta \right) \ln \left(\frac{m_1^2}{m_2^2} \right) \\ &- \frac{1}{2} \sqrt{1 - 2\Sigma + \Delta^2} \ln \left(\frac{1 - \Sigma + \sqrt{1 - 2\Sigma + \Delta^2}}{1 - \Sigma - \sqrt{1 - 2\Sigma + \Delta^2}} \right) \end{aligned} \quad (49)$$

with

$$\Sigma \equiv \frac{m_1^2 + m_2^2}{p^2}, \quad \Delta \equiv \frac{m_1^2 - m_2^2}{p^2}. \quad (50)$$

The function $F(p^2; m_1, m_2)$ vanishes in the limit $p^2 \rightarrow 0$. The general form of the \hat{C}_0 function is fairly complex and we refer the reader to Ref. [19]. The special case relevant for our calculations is

$$\begin{aligned} \hat{C}_0 [0, 0, Q^2; m_1, m_2, m_3] &= \frac{1}{(4\pi)^2} \int_0^1 dy \frac{1}{m_3^2 - m_1^2 - yQ^2} \\ &\times \ln \left[\frac{y(y-1)Q^2 + (m_2^2 - m_3^2)y + m_3^2}{y(m_2^2 - m_1^2) + m_1^2} \right]. \end{aligned} \quad (51)$$

B.2 Tensor Integrals

Definition and general form of B_1 :

$$\begin{aligned} B_\mu [p; m_1, m_2] &= i \mu^{4-d} \int \frac{d^d k}{(2\pi)^d} \frac{k_\mu}{(k^2 - m_1^2) [(k+p)^2 - m_2^2]} \equiv p_\mu B_1 [p^2; m_1, m_2], \\ B_1 [p^2; m_1, m_2] &= -\frac{1}{2} B_0 [p^2; m_1, m_2] + \frac{1}{(4\pi)^2} \left(\frac{m_1^2 - m_2^2}{2p^2} \right) F(p^2; m_1, m_2). \end{aligned} \quad (52)$$

Note the following useful relations among the B -functions:

$$\begin{aligned} 0 &= B_0 [p^2; m_1, m_2] + B_1 [p^2; m_1, m_2] + B_1 [p^2; m_2, m_1], \\ 0 &= (m_1^2 - m_2^2) B_0 [0; m_1, m_2] + (m_2^2 - m_3^2) B_0 [0; m_2, m_3] + (m_3^2 - m_1^2) B_0 [0; m_3, m_1]. \end{aligned} \quad (53)$$

Definition of the C –functions: (Note the difference from the definitions in Ref. [19].)

$$\begin{aligned}
C_\mu [p, q; m_1, m_2, m_3] &= i \int \frac{d^4 k}{(2\pi)^4} \frac{k_\mu}{(k^2 - m_1^2) [(k+p)^2 - m_2^2] [(k+q)^2 - m_3^2]} \\
&\equiv p_\mu \hat{C}_{11} + q_\mu \hat{C}_{12}, \\
C_{\mu\nu} [p, q; m_1, m_2, m_3] &= i \mu^{4-d} \int \frac{d^d k}{(2\pi)^d} \frac{k_\mu k_\nu}{(k^2 - m_1^2) [(k+p)^2 - m_2^2] [(k+q)^2 - m_3^2]} \\
&\equiv p_\mu p_\nu \hat{C}_{21} + q_\mu q_\nu \hat{C}_{22} + (p_\mu q_\nu + q_\mu p_\nu) \hat{C}_{23} + g_{\mu\nu} \hat{C}_{24}.
\end{aligned} \tag{54}$$

For the purpose of this paper, we will only need to evaluate these functions for $p^2 = q^2 = 0$ (we neglect final state fermion masses). $Q^2 = (p-q)^2 = -2p \cdot q$ will then be the invariant mass squared of the initial vector boson. For this parameter choice, the C –functions can be expressed in terms of the B –functions and \hat{C}_0 as:

$$\begin{aligned}
\hat{C}_{11} &= -\frac{1}{Q^2} \left\{ B_0 [0; m_1, m_2] - B_0 [Q^2; m_2, m_3] - (m_1^2 - m_3^2) \hat{C}_0 \right\}, \\
\hat{C}_{12} &= -\frac{1}{Q^2} \left\{ B_0 [0; m_1, m_3] - B_0 [Q^2; m_2, m_3] - (m_1^2 - m_2^2) \hat{C}_0 \right\}, \\
\hat{C}_{24} &= \frac{1}{2} \left[-B_1 [Q^2; m_2, m_3] + (m_1^2 - m_2^2) \hat{C}_{11} + m_1^2 \hat{C}_0 - \frac{1}{2(4\pi)^2} \right], \\
(d-2) \hat{C}_{24} - Q^2 \hat{C}_{23} &= -B_1 [Q^2; m_3, m_2] - (m_1^2 - m_2^2) \hat{C}_{11} + \frac{1}{2(4\pi)^2}. \tag{55}
\end{aligned}$$

We do not list expressions for \hat{C}_{21} nor \hat{C}_{22} since we do not use them in this paper.

B.3 Decoupling Limit

Below we list approximate formulas valid in the decoupling limit $p^2/m_{s,f}^2 \rightarrow 0$. Here m_s and m_f denote the scalar and fermion masses, respectively. Omitting the $\mathcal{O}(p^2/m_{s,f}^2)$ terms, we have

$$\begin{aligned}
[(d-2) \hat{C}_{24} - p^2 \hat{C}_{23}] (0, 0, p^2; m_s, m_f, m_f) &\approx -\frac{1}{(4\pi)^2} \left[\frac{1}{2} \left(\Delta_\epsilon - \ln \frac{m_f^2}{\mu^2} \right) + f(x) \right], \\
\hat{C}_{24} (0, 0, p^2; m_f, m_s, m_s) &\approx -\frac{1}{2(4\pi)^2} \left[\frac{1}{2} \left(\Delta_\epsilon - \ln \frac{m_f^2}{\mu^2} \right) - g(x) \right], \\
m_f^2 \hat{C}_0 (0, 0, p^2; m_s, m_f, m_f) &\approx -\frac{1}{(4\pi)^2} [f(x) + g(x)], \\
\hat{B}_1 (0; m_f, m_s) &\approx \frac{1}{(4\pi)^2} \left[\frac{1}{2} \left(\Delta_\epsilon - \ln \frac{m_f^2}{\mu^2} \right) - g(x) \right], \tag{56}
\end{aligned}$$

where

$$f(x) = -\frac{1}{4(1-x)^2} (x^2 - 1 - 2 \ln x),$$

$$g(x) = -\frac{1}{2} \ln x + \frac{1}{4(1-x)^2} \left[-(1-x)(1-3x) + 2x^2 \ln x \right] \quad (57)$$

for $x = m_f^2/m_s^2$.

References

- [1] H. N. Brown *et al.* [Muon g-2 Collaboration], Phys. Rev. Lett. **86**, 2227 (2001).
- [2] A. Czarnecki and W. J. Marciano, hep-ph/0102122.
- [3] F. J. Yndurain, hep-ph/0102312; K. Melnikov, hep-ph/0105267; see also W. J. Marciano and B. L. Roberts, hep-ph/0105056.
- [4] M. S. Chanowitz, hep-ph/9905478; hep-ph/0104024; J. H. Field and D. Sciarrino, Mod. Phys. Lett. A **15**, 761 (2000).
- [5] A. Gurtu, talk presented at *ICHEP 2000, Osaka, Japan, July 2000* (transparencies available at <http://ichep2000.hep.sci.osaka-u.ac.jp/plenary.html>); M. L. Swartz, in *Proc. of the 19th Intl. Symp. on Photon and Lepton Interactions at High Energy LP99*, ed. J.A. Jaros and M.E. Peskin, Int. J. Mod. Phys. A **15S1**, 307 (2000) [hep-ex/9912026].
- [6] O. Lebedev, W. Loinaz and T. Takeuchi, Phys. Rev. D **62**, 015003 (2000); O. Lebedev, W. Loinaz and T. Takeuchi, Phys. Rev. D **61**, 115005 (2000).
- [7] O. Lebedev, W. Loinaz and T. Takeuchi, Phys. Rev. D **62**, 055014 (2000).
- [8] L. N. Chang, O. Lebedev, W. Loinaz and T. Takeuchi, Phys. Rev. Lett. **85**, 3765 (2000).
- [9] L. N. Chang, O. Lebedev, W. Loinaz and T. Takeuchi, Phys. Rev. D **63**, 074013 (2001).
- [10] M. Carena, S. Heinemeyer, C. E. Wagner and G. Weiglein, hep-ph/0008023.
- [11] G. Cho and K. Hagiwara, hep-ph/0105037; G. Altarelli, F. Caravaglios, G.F. Giudice, P. Gambino, G. Ridolfi, hep-ph/0106029.
- [12] G. Cho and K. Hagiwara, Nucl. Phys. B **574**, 623 (2000); G. Cho, K. Hagiwara and M. Hayakawa, Phys. Lett. B **478**, 231 (2000); G. Altarelli, R. Barbieri and F. Caravaglios, Int. J. Mod. Phys. A **13**, 1031 (1998); G. Altarelli, R. Barbieri and F. Caravaglios, Phys. Lett. B **314**, 357 (1993); D. Garcia and J. Sola, Phys. Lett. B **357**, 349 (1995); D. Garcia, R. A. Jimenez and J. Sola, Phys. Lett. B **347**, 309 (1995); D. Garcia, R. A. Jimenez and J. Sola, Phys. Lett. B **347**, 321 (1995) [Erratum-ibid. B **351**, 602 (1995)]; Y. Yamada, K. Hagiwara and S. Matsumoto, Prog. Theor. Phys. Suppl. **123**, 195 (1996).
- [13] S. Bertolini, F. Borzumati, A. Masiero and G. Ridolfi, Nucl. Phys. B **353**, 591 (1991).
- [14] H. E. Haber and G. L. Kane, Phys. Rept. **117**, 75 (1985).
- [15] T. Takeuchi, A. K. Grant and J. L. Rosner, hep-ph/9409211; W. Loinaz and T. Takeuchi, Phys. Rev. D **60**, 015005 (1999).

- [16] M. E. Peskin and T. Takeuchi, Phys. Rev. Lett. **65**, 964 (1990); Phys. Rev. D **46**, 381 (1992).
- [17] K. Jakobs, talk presented at *XXXVIth Rencontres de Moriond, Les Arcs, France, March 2001* (transparencies available from <http://moriond.in2p3.fr/EW/2001/program.html>); D.E. Groom *et al.*, Eur. Phys. J. **C15**, 1 (2000).
- [18] S. P. Martin and J. D. Wells, hep-ph/0103067.
- [19] G. 't Hooft and M. Veltman, Nucl. Phys. **B153**, 365 (1979); G. Passarino and M. Veltman, Nucl. Phys. **B160**, 151 (1979).
- [20] W. F. L. Hollik, Fortschr. Phys. **38**, 165–260 (1990).
- [21] J. Mnich, CERN-EP/99-143; S. Fahey, G. Quest, talks presented at *EPS-HEP'99, Tampere, Finland, July 1999* (transparencies available from <http://neutrino.pc.helsinki.fi/hep99/>); K. Abe, *et al.* [SLD Collaboration], hep-ex/9908006; J. E. Brau [The SLD Collaboration], talk presented at *HEP EPS-99, Tampere, Finland, July 15 1999* (transparencies available from <http://www-sld.slac.stanford.edu/sldwww/pubs.html>); P. C. Rowson, private communication.
- [22] The ZFITTER package: D. Bardin, *et al.*, Z. Phys. **C44**, 493 (1989); Nucl. Phys. **B351**, 1 (1991); Phys. Lett. **B255**, 290 (1991); CERN-TH-6443/92, 1992; DESY 99-070, hep-ph/9908433.

Observable	Measured Value	ZFITTER Prediction
<i>Z</i> lineshape variables		
m_Z	91.1876 ± 0.0021 GeV	input
Γ_Z	2.4952 ± 0.0023 GeV	unused
σ_{had}^0	41.541 ± 0.037 nb	unused
R_e	20.804 ± 0.050	20.739
R_μ	20.785 ± 0.033	20.739
R_τ	20.764 ± 0.045	20.786
$A_{\text{FB}}(e)$	0.0145 ± 0.0025	0.0152
$A_{\text{FB}}(\mu)$	0.0169 ± 0.0013	0.0152
$A_{\text{FB}}(\tau)$	0.0188 ± 0.0017	0.0152
$R_{\nu/e}$	1.9755 ± 0.0080	1.9916
τ polarization at LEP		
A_e	0.1498 ± 0.0048	0.1423
A_τ	0.1439 ± 0.0042	0.1424
SLD left-right asymmetries		
A_{LR}	0.1514 ± 0.0022	0.1423
A_e	0.1544 ± 0.0060	0.1423
A_μ	0.142 ± 0.015	0.1423
A_τ	0.136 ± 0.015	0.1424

Table 2: LEP/SLD observables and their Standard Model predictions. The data are from Refs.[5] and [21]. The Standard Model predictions were calculated using ZFITTER v.6.21 [22] with $m_t = 174.3$ GeV, $m_H = 300$ GeV, and $\alpha_s(m_Z) = 0.120$ as input.

	m_Z	Γ_Z	σ_{had}^0	R_e	R_μ	R_τ	$A_{\text{FB}}(e)$	$A_{\text{FB}}(\mu)$	$A_{\text{FB}}(\tau)$
m_Z	1.000	-0.008	-0.050	0.073	0.001	0.002	-0.015	0.046	0.034
Γ_Z		1.000	-0.284	-0.006	0.008	0.000	-0.002	0.002	-0.003
σ_{had}^0			1.000	0.109	0.137	0.100	0.008	0.001	0.007
R_e				1.000	0.070	0.044	-0.356	0.023	0.016
R_μ					1.000	0.072	0.005	0.006	0.004
R_τ						1.000	0.003	-0.003	0.010
$A_{\text{FB}}(e)$							1.000	-0.026	-0.020
$A_{\text{FB}}(\mu)$								1.000	0.045
$A_{\text{FB}}(\tau)$									1.000

Table 3: The correlation of the Z lineshape variables at LEP. The correlation of $R_{\nu/e}$ with $A_{\text{FB}}(e)$ is +0.28, while its correlation with the μ and τ observables is negligible.

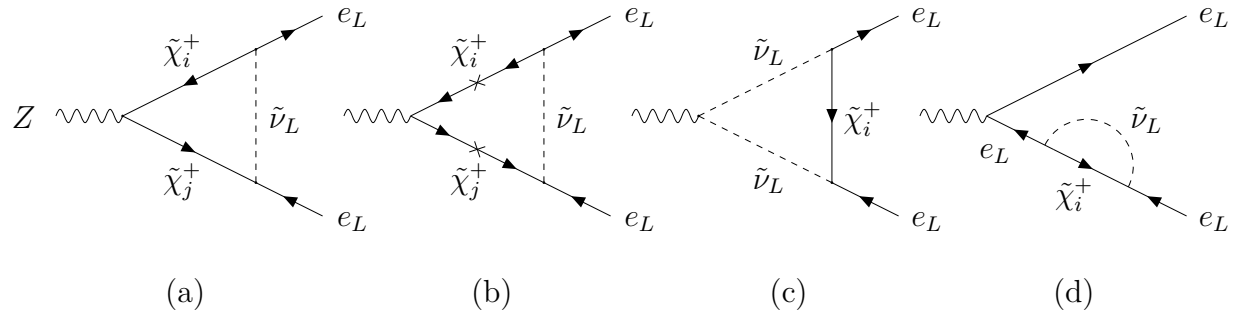


Figure 1: Chargino-sneutrino corrections to the $Ze_L\bar{e}_L$ vertex (in this and other figures the wave function renormalization diagram with a loop on the upper fermion leg is not shown).

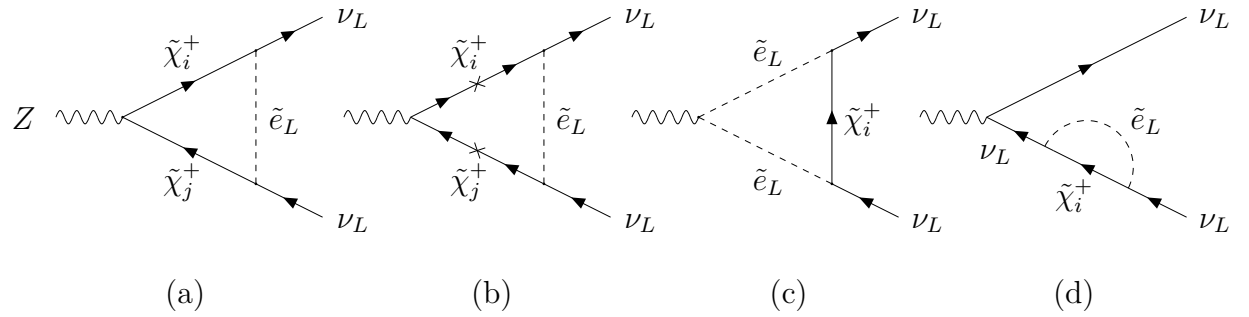


Figure 2: Chargino-selectron corrections to the $Z\nu_L\bar{\nu}_L$ vertex.

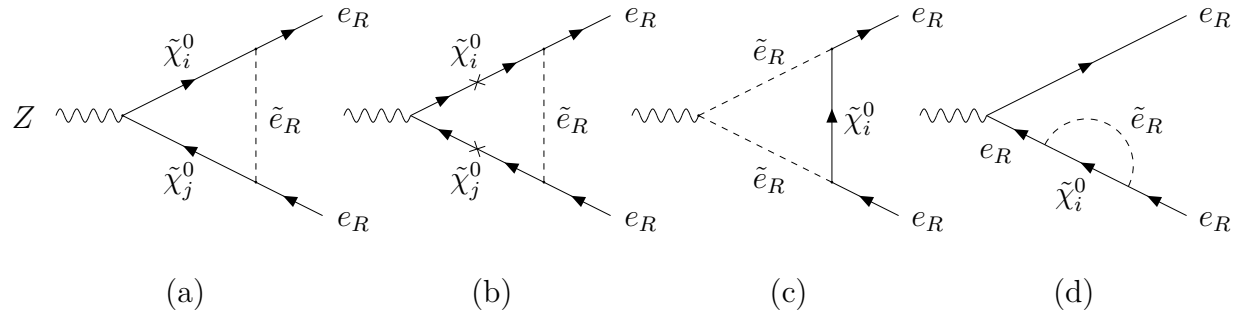


Figure 3: Neutralino-selectron corrections to the $Z e_R \bar{e}_R$ vertex.

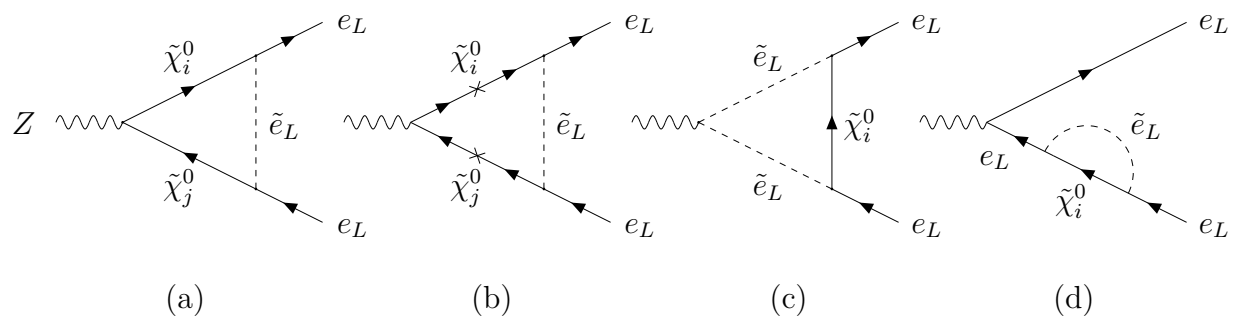


Figure 4: Neutralino-selectron corrections to the $Z e_L \bar{e}_L$ vertex.

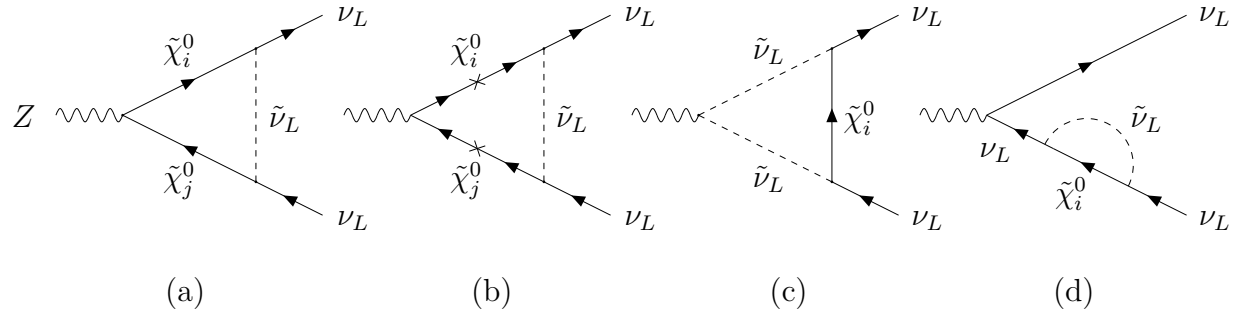


Figure 5: Neutralino-sneutrino corrections to the $Z\nu_L\bar{\nu}_L$ vertex.

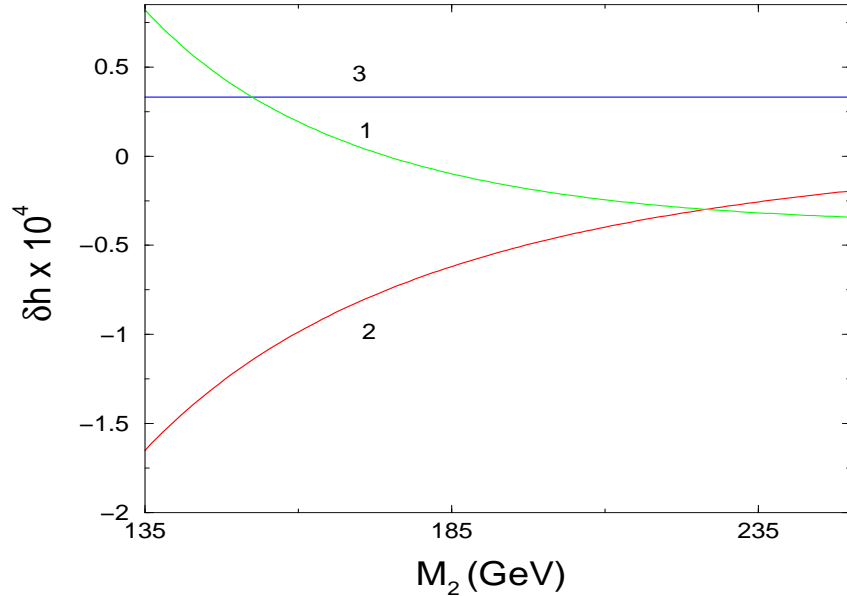


Figure 6: Vertex corrections to the $Z\bar{f}f$ couplings as a function of the GUT scale parameter M_2 for $\phi_\mu = 0$. 1 – δh_ν , 2 – δh_{e_L} , 3 – δh_{e_R} . The other GUT scale parameters are $m_{\tilde{l}} = 10$ GeV, $m_{\tilde{e}} = 85$ GeV, $M_1 = 100$ GeV, $M_3 = 200$ GeV, $A = 100$ GeV, $\tan\beta = 3$. The other scalar mass parameters are set to 100 GeV and the CP-phases are set to zero.

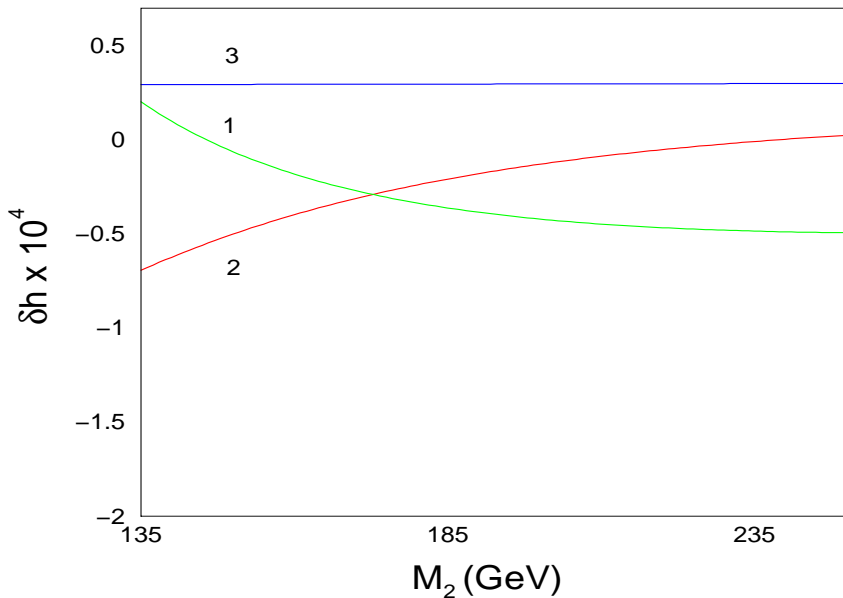


Figure 7: Vertex corrections to the $Z\bar{f}f$ couplings as a function of the GUT scale parameter M_2 for $\phi_\mu = \pi$. 1 – δh_ν , 2 – δh_{e_L} , 3 – δh_{e_R} . The other GUT scale parameters are $m_{\tilde{l}} = 10$ GeV, $m_{\tilde{e}} = 85$ GeV, $M_1 = 100$ GeV, $M_3 = 200$ GeV, $A = 100$ GeV, $\tan \beta = 3$. The other scalar mass parameters are set to 100 GeV and the CP-phases are set to zero.

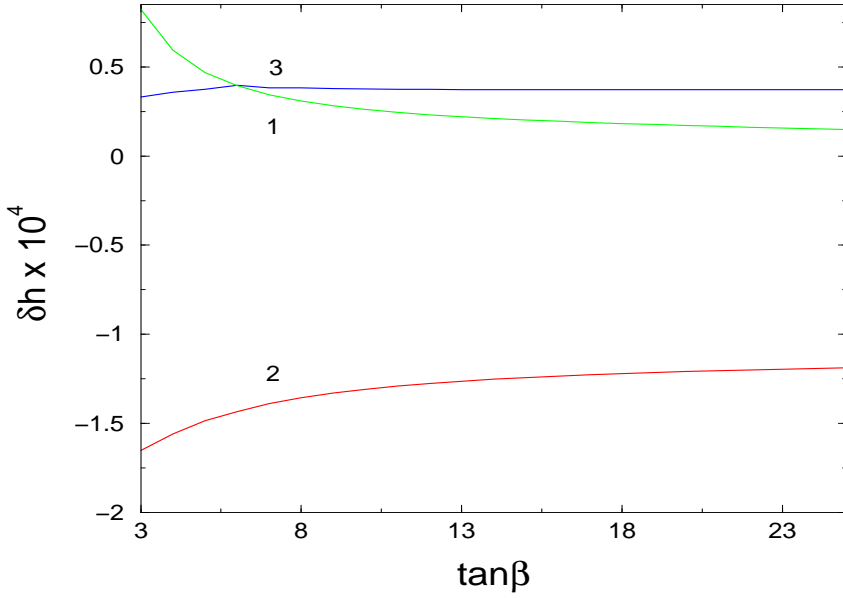


Figure 8: Vertex corrections to the $Z\bar{f}f$ couplings as a function of $\tan\beta$ for $\phi_\mu = 0$. 1 – δh_ν , 2 – δh_{e_L} , 3 – δh_{e_R} . The other GUT scale parameters are $m_{\tilde{l}} = 10$ GeV, $m_{\tilde{e}} = 85$ GeV, $M_1 = 100$ GeV, $M_2 = 135$ GeV, $M_3 = 200$ GeV, $A = 100$ GeV. The other scalar mass parameters are set to 100 GeV and the CP-phases are set to zero.

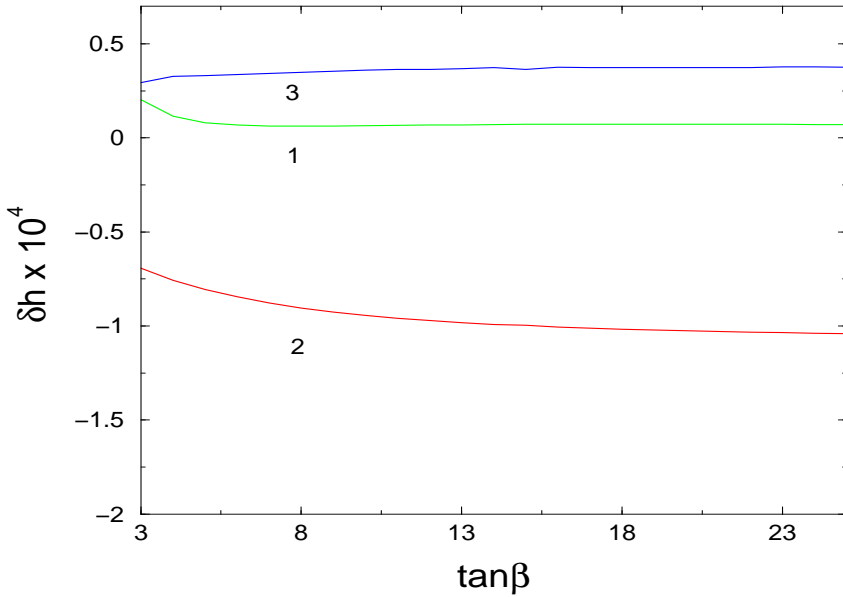


Figure 9: Vertex corrections to the $Z\bar{f}f$ couplings as a function of $\tan\beta$ for $\phi_\mu = \pi$. 1 – δh_ν , 2 – δh_{e_L} , 3 – δh_{e_R} . The other GUT scale parameters are $m_{\tilde{l}} = 10$ GeV, $m_{\tilde{e}} = 85$ GeV, $M_1 = 100$ GeV, $M_2 = 135$ GeV, $M_3 = 200$ GeV, $A = 100$ GeV. The other scalar mass parameters are set to 100 GeV and the CP-phases are set to zero.

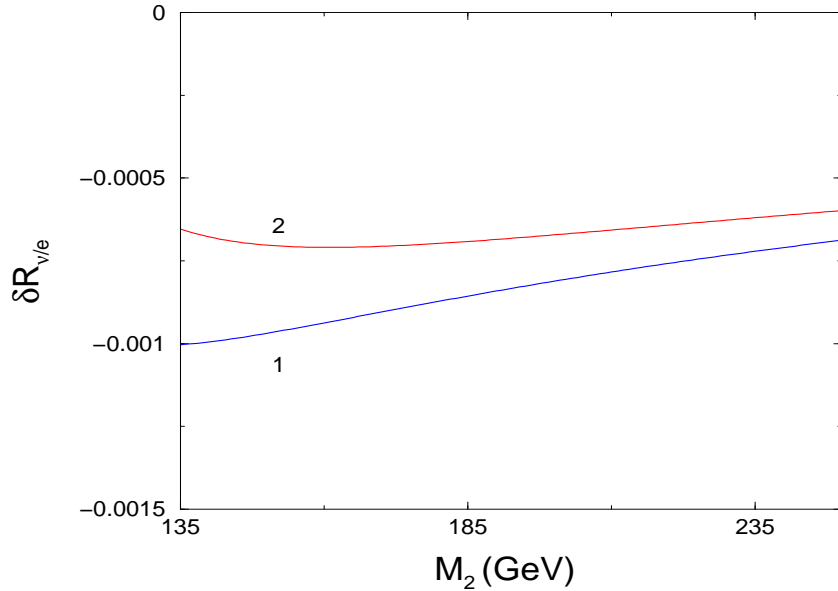


Figure 10: Shift in $R_{\nu/e}$ due to the vertex corrections as a function of M_2 (this corresponds to the range of the light chargino mass from 95 to 180 GeV). 1 – $\phi_\mu = 0$, 2 – $\phi_\mu = \pi$. The GUT scale parameters are $m_{\tilde{l}} = 10$ GeV, $m_{\tilde{e}} = 85$ GeV, $M_1 = 100$ GeV, $M_3 = 200$ GeV, $A = 100$ GeV, $\tan \beta = 3$.

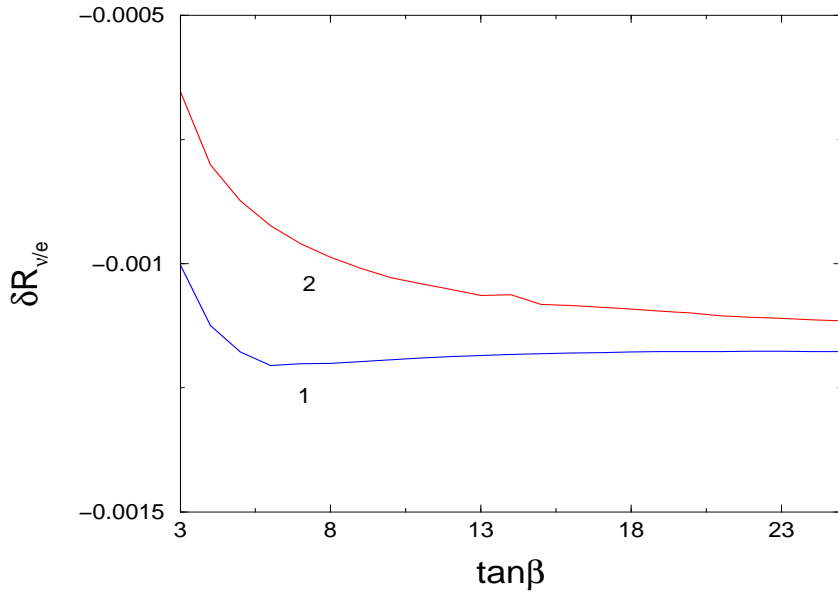


Figure 11: Shift in $R_{\nu/e}$ due to the vertex corrections as a function of $\tan \beta$. 1 – $\phi_\mu = 0$, 2 – $\phi_\mu = \pi$. The GUT scale parameters are $m_{\tilde{l}} = 10$ GeV, $m_{\tilde{e}} = 85$ GeV, $M_1 = 100$ GeV, $M_2 = 135$ GeV, $M_3 = 200$ GeV, $A = 100$ GeV.

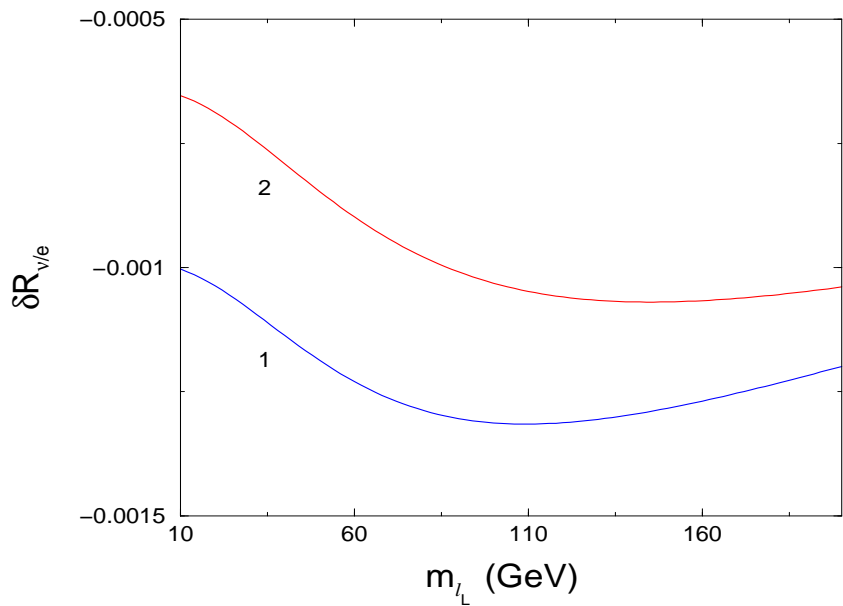


Figure 12: Shift in $R_{\nu/e}$ due to the vertex corrections as a function of the GUT scale slepton mass parameter $m_{\tilde{l}}$ (this corresponds to the range of the slepton mass $m_{\tilde{e}_L}$ from 104 to 225 GeV). $1 - \phi_\mu = 0$, $2 - \phi_\mu = \pi$. The other GUT scale parameters are $m_{\tilde{e}} = 85$ GeV, $M_1 = 100$ GeV, $M_2 = 135$ GeV, $M_3 = 200$ GeV, $A = 100$ GeV, $\tan \beta = 3$.